Experimental Study on the Structural Performance of Shear Panel Dampers Under Constant Vertical Deformation

I. Suzuki, S. Sasaki, D. Katsura & K. Tahara
Fujita Corporation, Tokyo

SUMMARY:
Seismic shear panel dampers installed in the middle of span of structural frame by conventional construction procedures have compressive axial load and strain caused by dead and live loadings. In the case of a structural frame consisting of reinforced concrete members, the panel damper is subjected to additional compressive strain caused by shrinking and creep of the reinforced concrete columns. On the other hand, the geometrical displacement of the damper in the vertical direction with shear deformation is restricted by structural frame. It is considered that the panel damper has axial tensile stress caused by this restriction at large shear deformation. So it is important to verify the influence of the initial vertical strain and restriction by the structural frame at the shear drift for optimal seismic design of the panel damper.
In this study, cyclic loading tests of the shear panel damper with initial vertical strain under fixed boundary conditions for vertical displacement were conducted. Based on the test results, the influence of initial strain and vertical fixed condition on shear strength and deformation capacity were investigated.

Keywords: shear panel damper, hysteretic damper, low yield strength steel, vertical deformation, axial force

1. INTRODUCTION

Shear panel dampers with low yield strength steel are generally installed on structural frames in the middle of a span with supporting members. There are three factors causing axial strain to damper. Firstly, the dampers sustain a part of the vertical load of building such as fixed and live load and have compressive strain. In steel structures, to decrease vertical stress on the shear panel damper, those dampers are connected to the frame after the steel erection work and casting of concrete floor slab on the construction site. In the case of structural frame consisting of reinforced concrete members, the dampers are installed simultaneously with the frame construction. Secondly, owing to shrinking and creep of the reinforced concrete columns, the axial compressive strain of the damper increases. The shrinking and creep strain are larger in the lower storeys of high-rise buildings with high-strength concrete. Thirdly, with shear deformation, the geometrical displacement of the damper for vertical direction is restricted by the structural frame. It is considered that panel dampers have axial tensile stress caused by this restriction at large shear deformations. To estimate the structural performance of the damper accurately, it is necessary to clarify the influence of vertical loading, compressive strain and vertical restriction.

Several previous experiments have been conducted on the seismic behaviour of shear panel dampers under constant vertical loading [Ohta, 2004 et al.]. It was reported that the deformation capacity of panel dampers under the constant vertical compressive loading was reduced compared to when under no load. However, in these studies, the influence of the restriction by the structural frame on the structural behaviour of panel damper at large shear deformation was not taken into consideration.

In this study, in order to verify the influence of initial vertical load, initial compressive strain and restriction by structural frame on the seismic behaviour of panel dampers, the static cyclic loading tests of shear panel dampers with initial vertical load and compressive strain under fixed vertical displacement were conducted.

2. OUTLINE OF EXPERIMENT

2.1. Shear Panel Specimen

The specimens tested were 2/3 the scale of a full-scale shear panel damper. The outline of the five specimens is listed in Table 1 and their configurations are shown in Figure 1. The shear panel dampers were composed of a low yield strength steel web panel, two flanges and two end plates. The web panel is stiffened by cross rib-plates. The width-thickness ratio of the flanges is 5.6, except for specimen DT-Z-S2, which has a ratio of 9.8. The mechanical properties of the steel used for the specimens are shown in Table 2

Table 1. List of Shear Panel Specimens

Specimen	Vertical boundary condition and initial strain	Type	Section	$(d/tw)_{eq}$ *1	b/t_f	Height [mm]
D-Z-S2	Fixed at 2% Compressive strain	D	H-468x134x6x12	28.3	5.6	268
D-Z-S0	Fixed at 0% strain	D				
D-Z+S004	Fixed at 0.04% tensile strain	D				
D-Z-0	Free	D				
DT-Z-S2	Fixed at 2% Compressive strain	DT	H-462x176x6x9		9.8	

*1 Equivalent width-thickness ratio calculated using Eqn. (2.1)

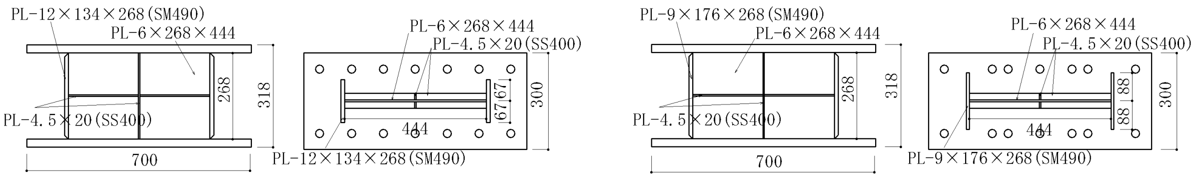

(a) Elevation (b) Cross section
(1) D-Series

(a) Elevation (b) Cross section
(2) DT-Series

Figure 1. Configurations of shear panel specimen

Table 2. Mechanical Properties

Specimen	Part	Steel grade	Thickness(measured) (mm)	σ_y (N/mm²)	σ_u (N/mm²)	elong. (%)
Common	Panel	LY225	9 (9.3)	250	333	50.9
D	Flange	SM490A	12 (11.9)	423	527	41.9
	Rib	SS400	4.5 (4.6)	332	454	34.8
DT	Flange	SM490A	9 (9.3)	363	522	38.1
	Rib	SS400	4.5 (4.5)	348	445	32.0

The experimental parameters are initial vertical strain and width-thickness ratio of the flanges. Four types of initial vertical strain (shown in Table 1) were introduced to the specimen and kept during horizontal loading. Specimen D-Z-S2 and DT-Z-S2 were given 2% of initial vertical compressive strain. D-Z-S0 and D-Z-0 were not given initial vertical strain. D-Z+S004 was given 0.04 % of tensile strains. In every specimen except for D-Z-0, the boundary condition for the vertical displacement was fixed, including the geometrical vertical displacement with shear deformation.

It is generally known that width-thickness ratio of the panels is an important factor in predicting the maximum strength and deformation capacity of shear panels. The equivalent width-thickness ratio with rib-plates is defined as the width-thickness ratio of square-shaped shear panels that have equivalent elastic shear buckling strength. In this study, the equivalent width-thickness with rub-plates was calculated by Eqn. 2.1.

$$\left(\frac{d}{t_w}\right)_{eq} = \sqrt{\frac{9.34\pi^2 E}{12\left(1-\nu^2\right)} \cdot \frac{1}{\tau_{cr}}} \tag{2.1}$$

Where, τ_{cr} is elastic shear buckling strength. (τ_{cr} is calculated from buckling eigenanalysis by finite element method in this paper.)

2.1. Test Apparatus

The test apparatus is shown in Figure 2. The shear panel specimen is set at loading blocks. Assuming seismic loading condition, the specimens are tested under cyclic horizontal loadings with gradually increasing amplitude. Prior to the horizontal loading of a specimen, the vertical displacement for initial strain was given and the vertical displacement was kept constant at horizontal loading except for D-Z-0. D-Z-0 has no vertical restriction at horizontal loading. The axial force and axial strain relationships prior to horizontal loading are shown in Figure 3. The measurement points of displacement and strain are shown in Figure 4.

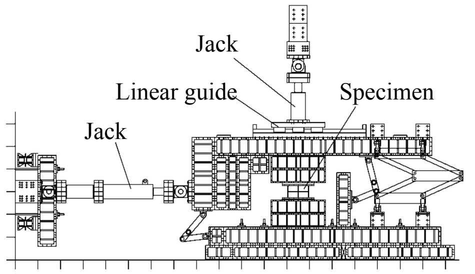

Figure 2. Test apparatus

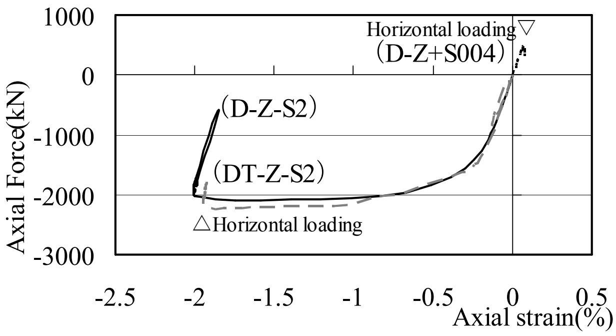

Figure 3. Axial force and axial strain relationship

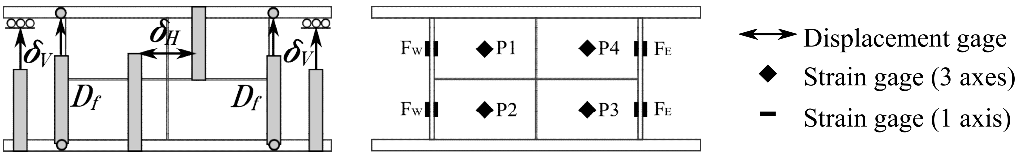

Figure 4. Measurement points of deformation and strain

3. TEST RESULTS

3.1. Test Results and Failure Mode

The test results are listed in Table 3. The shear force excludes additional shear caused by the P-Δ effect of vertical force. The yield strength is obtained by 0.35% offset method [BRI, 2002 et al.]. The failure mode of D-Z-S2 before horizontal loading is shown in Figure 5(a) and after horizontal loading in Figure 5(b). The panels and flanges yielded and out-of-plane deformation was generated by applying vertical strain. However, the out-of-plane deformation of flanges became unclear after horizontal loading. DT-Z-S2, which has same initial strain as D-Z-S2, showed similar deformation. The width-thickness ratio of the flanges did not appear to influence out-of-plane deformation. In every specimen, the shear buckling of panels occurred due to repetition of large shear deformation. Finally, the shear crack occurred near to the fillet welding of the shear panel to flange and the end-plate.

Table 3. Test Results

Specimen	Yield				Maximum (Up: Plus, Down: Minus)			Ultimate state	
	Exp.			Cal.	Exp.		Cal.[*4]	Exp.	Cal.[*4]
	Q_y [kN]	τ_y[*1] [N/mm^2]	γ_y 10^{-3}[rad]	τ_y[*2] [N/mm^2]	Q_{MAX} [kN]	τ_{pu}[*3] [N/mm^2]	τ_{pu} [N/mm^2]	$_c\gamma_u$ [rad]	$_c\gamma_u$ [rad]
D-Z-S2	404	148	1.9	144	725 -717	265 -262	272	- 1.52	1.84
D-Z-S0	357	131	1.7		765 -770	280 -282		- 1.52	
D-Z+S004	358	131	1.7		754 -759	276 -277		1.68 -	
DT-Z-S2	391	143	1.9		679 -681	250 -250		1.80 -	
D-Z-0	361	132	1.7		756 -767	276 -280		1.54 -	

*1 $\tau_y = Q_y/(b_w t_w)$, *2 $\tau_y = \sigma_y/\sqrt{3}$, *3 $\tau_{pu} = (Q_{\max} - Q_{fu})/(b_w t_w)$, *4 Calculated by Eqn. (4.4)

Where b_w is distance between the centers of both flanges and t_w is thickness of the panel.
Q_{fu} is the calculated shear loading capacity of the flanges, assuming plastic hinges at both flanges.

(a)Under initial vertical strain (b)After horizontal loading

Figure 5. Specimen photograph

3.2. Shear Force and Shear Drift Angle Relation

Relationships between shear force and shear drift angle (γ) are shown in Figure 6. Hysteresis curves of the panel dampers are spindle shapes and stable until shear cracking occurs at the fillet welding of the panel. The synthetic curves of relationships between shear force and drift angle are shown in Figure 7 [Kato and Akiyama, 1968]. The specimens with width-thickness ratios of 5.6 showed similar synthetic curves. Specimen DT-Z-S2, with a width-thickness ratio of 9.8, showed relatively low stiffness after the shear yielding of panel.

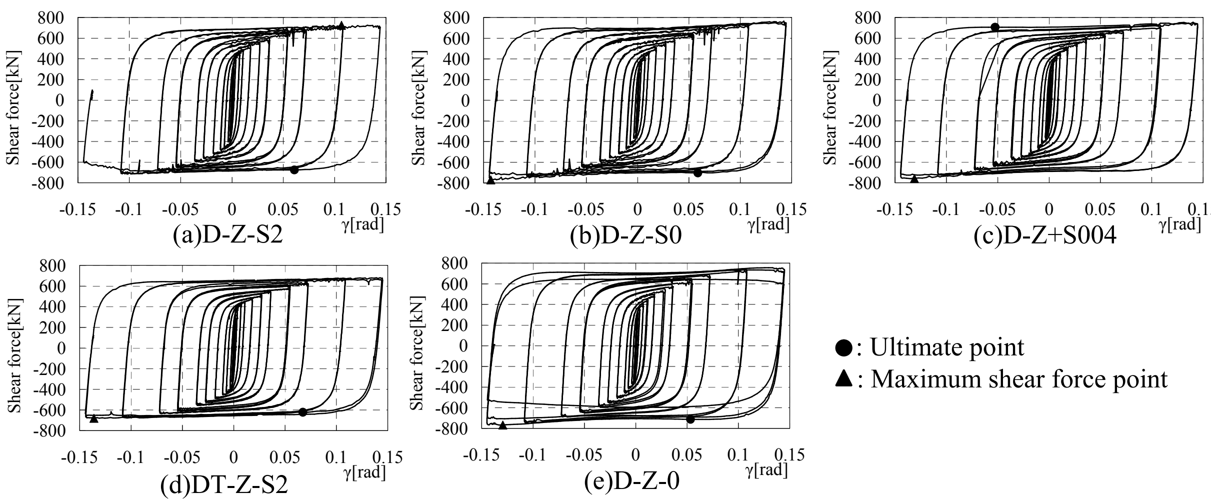

Figure 6. Relationships of shear force and shear drift angle

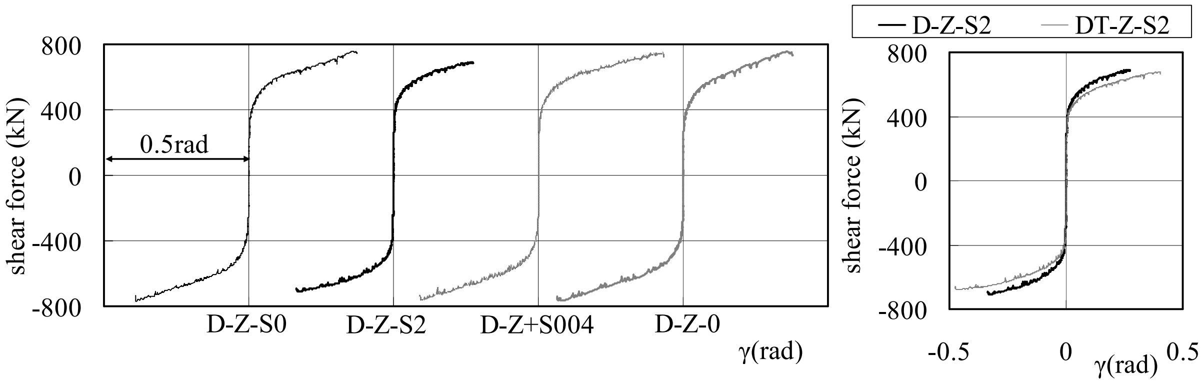

Figure 7. Synthetic curves of shear force and shear drift angle relationships

3.3. Shear Force and Cumulative Shear Drift Angle Relation

Relationships between the shear force and cumulative shear drift angle (γ_c) are shown in Figure 8. The reduction of shear force did not occur until the maximum shear strength in large cumulative shear drift angle. The influence of initial strain and restriction of vertical displacement was not observed on cumulative deformation until maximum strength.

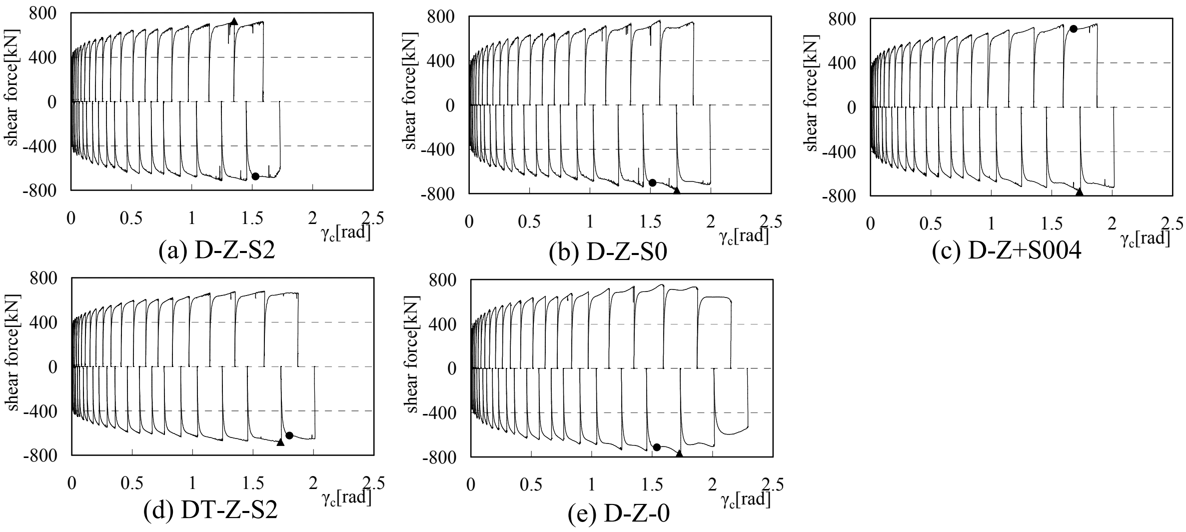

Figure 8. Relationships of shear force versus cumulative shear drift angle

3.4. Vertical Force and Shear Drift Angle Relation

Relationships between the vertical force and shear drift angle (γ) are shown in Figure 9. The tensile axial yield force of flanges (N_{fy}) is also shown in the figure. In case of specimen D-Z-S0 with vertical restriction with no initial strain, vertical force was small at small shear deformation. Owing to repetition of large horizontal loading, the compressive force occurred in a small range of shear drift angle. And the tensile force occurred in large range of shear drift angle. In the case of specimen D-Z+S004 that has 0.04% of tensile strain and vertical restriction, the initial tensile force decreased gradually. Thereafter, D-Z+S004 displayed similar behaviour to D-Z-S0.

In the case of specimen D-Z-S2 and DT-Z-S2 with 2% of compressive strain and vertical restriction, the compressive force was larger at small shear deformation. However it decreased gradually with horizontal loading. From 0.05 rad. of the loading cycle, both specimens displayed similar behaviour to D-Z-S0. Regardless of initial strain, the maximum vertical forces at large horizontal loading were approximately the same in every specimen.

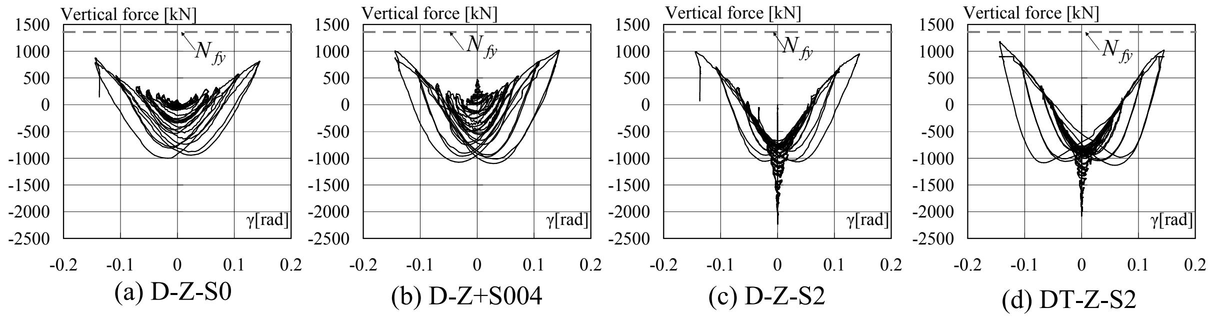

Figure 9. Relationships of vertical force and shear drift angle

Relationships between shear drift angle (γ) and the ratio of axial (δ_v) and vertical (D_f) displacement to the height of specimen (h) are shown in Figure 10. In case of specimen D-Z-0 with no initial strain and no vertical restriction, D_f/h gradually increases to tensile direction with cyclic horizontal loading. It seems that diagonal tension of web panel and plastic elongation of flanges were occurring. The shear panel damper had vertical displacement (D_f) caused by geometric deformation at the larger shear deformation, as shown in Figure 10(a).

The relationships of specimen D-Z-S0 with vertical restriction were shown in Figure 10(b). In case of specimen D-Z-S0, δ_v/h was constant, and D_f/h became larger with shear deformation increasing. It seems that D_f exceeded displacement of yielding for the axial direction. After plastic residual elongation occurred, the panel damper was subjected to compressive force at small shear drift angle, as shown in Figure 9. In addition the panel damper was subjected to tensile force at large shear drift angles. This behaviour occurred due to the restriction of geometric vertical deformation. These vertical forces became relative large, because the initial axial force had decreased at large horizontal loading. Thereafter, vertical force fluctuated with shear deformation. The amount of vertical force does not depend on initial vertical strain.

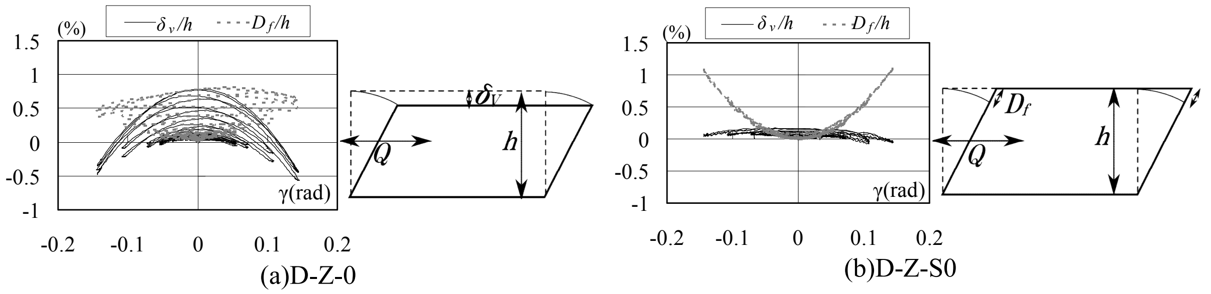

Figure 10. Relationships of shear drift angle and the rate of axial and vertical displacement

3.5. Axial Force of Each Part

Figure 11 show relationships between axial forces on dampers, panels and flanges and shear drift angle at the peak of the respective loading cycles. Axial force on the panel was given by measurements of strain gauges using plastic flow theory. Axial force on the flanges was calculated by subtracting that of panel from that of forces total.

In the case of specimens (a) D-Z+S004 and (b) D-Z-S2 with initial strain, the panels sustained initial axial force at small shear drift angle. However, with shear drift angle increasing, the axial force of panel decreased immediately to small and constant. It seems that the axial forces were transferred from the panel to the flanges. In the case of specimens (c) D-Z-S0 and (d) D-Z-0 with no initial strain, axial force of the panel was still small with shear drift angle increasing. The flanges were subjected to the axial force caused by large shear deformation.

Relationships between shear force (Q), axial force on the panel (N_p) and shear drift angle (γ) at the peak of respective loading cycles are shown in Figure 12. Shear yield strength (Q_y) is also shown in figure. Axial force on the panel was very small, when panel damper was shear yielding. Thereafter, axial force on the panel was approximately 0.

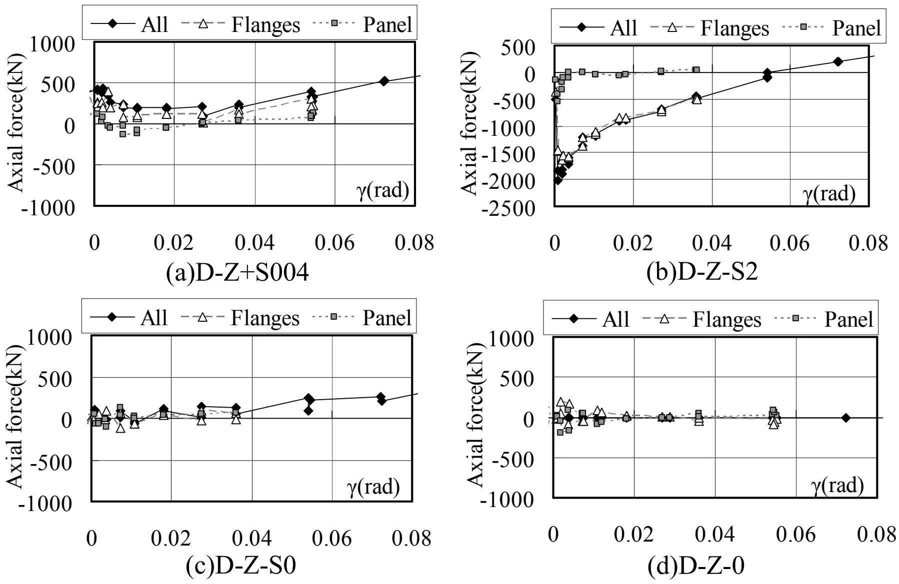

Figure 11. Axial force of each part

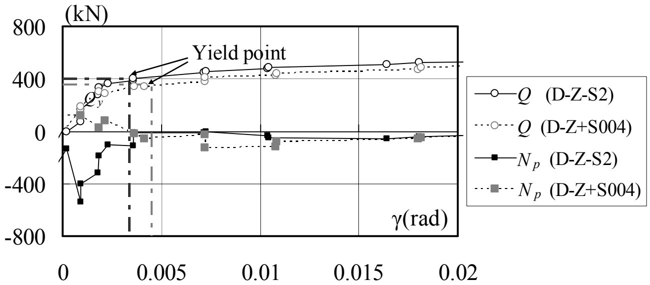

Figure 12. Shear force and axial force of panels

4. SHEAR STRENGTH AND EVALUATION OF DEFORMABILITY

4.1. Shear Yield Strength

Figure 13 shows a comparison between experimental and calculated yield (τ_y) and maximum (τ_{pu}) strength. Experimental results of shear yield strength agree with calculated values using results of material test without consideration of axial stress. This seems to be due to the fact that axial force on the panel was small at shear yielding, as had been pointed out. The influence of width-thickness ratio of flanges was not observed on experimental results of shear yield strength.

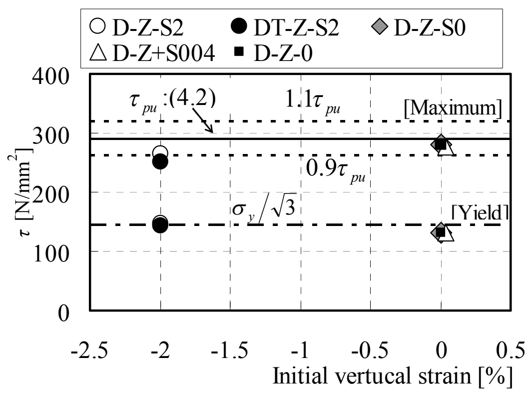

Figure 13. Yielding and maximum shear stress

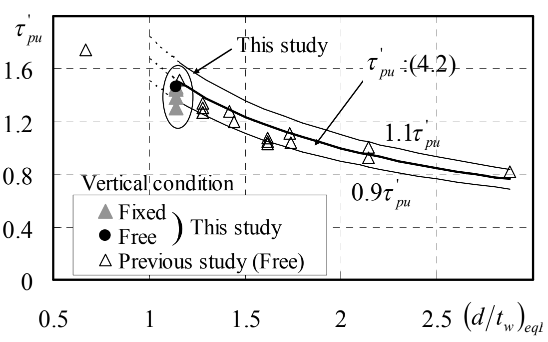

Figure 14. Comparisons of strength increase rate

4.2. Maximum Shear Strength

In case of specimen with initial compressive strain, experimental results of maximum shear strength shown in Figure 13 were smaller than the others. Specimen DT-Z-S2 with a width-thickness ratio of flange of 9.8 had lower maximum strength than D-Z-S2 with a width-thickness ratio of 5.6. The calculated values of maximum shear stress (τ_{pu}) in Figure 13 can be calculated by under Eqn. 4.1 – 4.3, where $(d/t_w)_{eqB}$ is modified width-thickness ratio [Tanaka and Sasaki, 2000]. The experimental results approximately agreed with calculated values.

$$\tau_{pu} = \tau_{pu}' \cdot \tau_B = 1.671 \left\{ (d/t_w)_{eqB} \right\}^{-0.741} \cdot \tau_B \tag{4.1}$$

$$(d/t_w)_{eqB} = (d/t_w)_{eq} \cdot \sqrt{\sigma_B / E} \tag{4.2}$$

$$\tau_B = \sigma_B / \sqrt{3} \tag{4.3}$$

Where, σ_B is ultimate tensile strength of material. τ_B is ultimate shear strength, E is Young's modulus, τ_{pu}' is strength increase rate.

Comparisons of strength increase rate (τ_{pu}') between experimental and previous results are shown in Figure 14. The previous results and empirical equation were given under no vertical restriction. As shown in this figure, τ_{pu}' of specimen with initial vertical strain can be evaluated by this equation.

4.3. Ultimate Cumulative Shear Drift Angle

Relationships between ultimate cumulative shear drift angle (${}_C\gamma_u$) and initial vertical strain are shown in Figure 15. The calculated values in the figure were calculated with Eqn. 4.4 using a modified width-thickness ratio [Tanaka and Sasaki, 2000]. The influence of initial strain was not observed in ${}_C\gamma_u$, except for specimen D-Z+S004 and DT-Z-S2. In case of specimen D-Z+S004, ${}_C\gamma_u$ was slightly larger than the others. On the other hand, in case of specimen DT-Z-S2 with larger width-thickness ratio of flanges, ${}_C\gamma_u$ was larger than for D-Z-S2.

Figure 16 shows the relationships between ${}_C\gamma_u$ and modifies width-thickness ratio with previous results without vertical restriction. The calculated value of ${}_C\gamma_u$ by Eqn. 4-4 is shown in this figure. Ultimate cumulative shear drift angle of specimen with initial vertical strain can be evaluated by empirical equation proposed previously under no vertical restriction.

$${}_C\gamma_u = 2.936 \left\{ (d/t_w)_{eqB} \right\}^{-3.569} \tag{4.4}$$

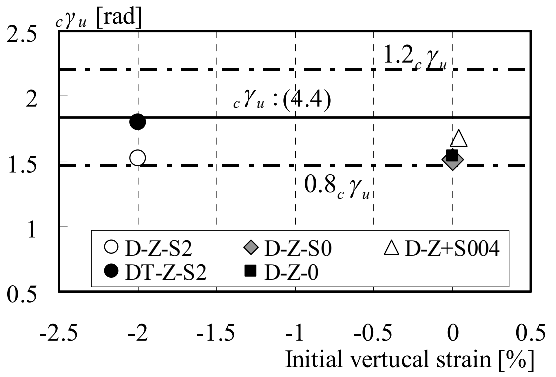

Figure 15. Ultimate cumulative shear drift angle and initial vertical strain relationships

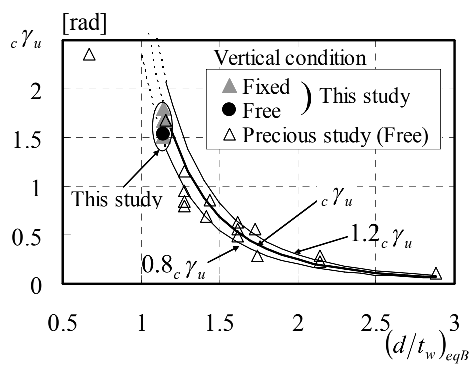

Figure 16. Comparisons of ultimate cumulative shear drift angle

5. CONCLUSIONS

Static loading tests of shear panel damper with low yield strength steel under fixed vertical displacement were conducted. Our conclusions are as follows:
(1)Hysteric performances of shear panel dampers with vertical restriction and initial strain did not differ significantly from those without vertical restriction.
(2)Axial force of panel decreases immediately with shear deformation introduced. Under restriction of vertical deformation, axial force fluctuated due to cyclic shear loading. The reason is that flanges were subjected to that axial force and web is free from that.
(3) After shear yielding of the damper, the hysteretic performance of the damper was stable, because the web panel did not sustain the vertical load.
(4) The maximum shear strength and ultimate cumulative shear drift angle of the damper can be predicted exactly by the previous empirical equation.

REFERENCES

Tanaka, K., and Sasaki, Y. (2000). Hysteretic performance of shear panel dampers of ultra low-yield-strength steel for seismic response control of buildings. 12th *World confference of eartquake engineering*, 1248.
Tanaka, K., Torii, T., Sasaki, Y., Miyama, T., Kawai, H., Iwata, M. and Wada, A. (1998b). Practical application of damage tolerant structures with seismic control panel using low-yield-point steel to a high-rise steel building, *Proceedings of SEWC*, San Francisco, USA, T190-4.
Ohta, Y., and Kaneko, H., Kibayashi, M., Yamamoto, M., Muroya, T, and Nakane, K., (2004). Study on shear panel dampers using low yield strength steel applied to reinforced concrete buildings. 13th *World confference of eartquake engineering*, 2228.
Akiyama, H., and Kato, B., (1968).The ultimate strength od the steel beam-column part 4. *Journal of Structural and Construction Engineering,* **No.151**, pp.15-20, in Japanese
BRI (Building research institute) and Japan iron and steel federation. (2002). Report of testing methods of the evaluation of structural performance for the steel structures, Building research institute and Japan iron and steel federation, in Japanese